

AN EXTENDED 1-D TRANSIENT CORROSION MODEL INCLUDING MULTI-COMPONENT CHEMICAL SPECIES

M. P. Baral¹, B. W. Karney², G. Naser³ and A. Colombo⁴

1. Graduate Student, Civil Engineering Department, University of Toronto, Toronto, ON, Canada, E-mail:<madhav.baral@gmail.com>
2. Professor, Civil Engineering Department, University of Toronto, Toronto, ON, Canada, E-mail:<karney@ecf.utoronto.ca>
3. Graduate Student, Civil Engineering Department, University of Toronto, Toronto, ON, Canada, E-mail:<ghnaser@yahoo.com>
4. Research Associate, Civil Engineering Department, University of Toronto, Toronto, ON, Canada, E-mail:< andrew.colombo@utoronto.ca>

Abstract

Corrosion in a water distribution system has many adverse impacts including the build-up of scale on the pipe wall, the loss of hydraulic capacity, compromised structural integrity that can lead to the onset and proliferation of leakage, and the deterioration of water quality. Yet, for all its familiarity, pipe corrosion is a complex phenomenon due to the inter-dependent set of reactions that can take place at the pipe wall and with chemicals in the bulk water. The principle objective of this study is to explore the impact of chemical species on an existing but basic 1-D transient model. The research is focused on studying the impact of various chemical species – dissolved oxygen, pH, and the carbonate system (CO_2 , HCO_3^- , & CO_3^{2-}) on the formation of ferrous (Fe^{2+}) and ferric (Fe^{3+}) ions. The associated formation of various iron precipitates is also numerically explored. For the purpose of this study, the 1-D corrosion simulation model developed by Naser and Karney (2005) is extended by adding three sets of chemical reactions including reaction of the pipe wall with the bulk water and dissolved oxygen, reactions involving the carbonate system, and iron precipitation. Each chemical species is tracked using the advection-diffusion-reaction equation (ADRE) coupled to a hydraulic model involving the continuity and momentum equations. The numerical solution of ADRE is computed by the implicit finite difference method and the flow equations are resolved with the method of characteristics (MOC).

The model is simulated for various flow conditions both with and without consideration of the carbonate system. Results show that the rate of iron release increases in the axial direction but varies with flow conditions and simulation time. When the carbonate system is neglected, the oxygen concentration steadily decreases, and both iron concentrations and pH increase along the pipe axis with time. However, the inclusion of the carbonate system directly affects the pH and dissolved oxygen concentration in the bulk water which then influences the rate of iron release. In particular, the decrease in pH values and the increase in dissolved oxygen concentrations along the pipe axis, which are observed by the inclusion of the carbonate system into the model, accelerate oxidation of the pipe wall, and a high rate of iron release is observed. This reveals that flow conditions, low pH, high dissolved oxygen concentrations, are the most significant factors that increase the corrosion rate. In a real water distribution system, the rate of internal corrosion is further influenced by other so-called secondary reactions, and also by the physical, chemical and biological characteristics of the water.

Keywords

Pipe corrosion, Transient flow, 1-D model, Iron release, Finite difference method

1. INTRODUCTION

Pipe corrosion is a major problem associated with distribution network aging and microbial activity, which may progress internally and externally. External corrosion has direct implications for pipe longevity, while internal corrosion can also restrict the water carrying capacity of a pipe and cause discolouration of the water, a deterioration in water quality, and a reduction in disinfectant residual. Internal corrosion is a complex phenomenon due to reactions between the pipe wall and bulk water. The AWWA Research Foundation has studied in detail the corrosion of iron and steel pipes, its impact on water quality and possible remedial measures (Benjamin et al., 1996). McNeill and Edward (2001) mentioned three distinct corrosion related problems: loss of pipe mass through oxidation to soluble iron species, increase of headloss and decrease of water carrying capacity due to scale accumulation or tuberculation, and a decrease in the aesthetic quality of water. Tubercle deposits are attractive habitats for microbial colonization. Internal corrosion can be influenced by the physical, chemical and biological characteristics of the water arises through several different mechanisms, such as high turbulent flow velocities that erode the surface of the pipe and chemical dissolutions that remove wall material to the bulk flow. Significant factors responsible for an elevated corrosion rate include DO, pH, water flow characteristics (turbulence, mixing, changes in flow velocity and pressure due to transient shear stress), pipe diameter, pipe wall conditions, temperature, water treatment practices, total carbonate concentration, suspended solids, organic matters, anions (such as Cl^- , SO_4^{2-} , PO_4^{3-} , SiO_2 , etc.), and biological factors can influence the internal corrosion of new/old iron pipes in water distribution systems (Geldreich, 1996; Benjamin et al., 1996; Grayman et al., 2000; Sarin et al., 2001).

In a water distribution system, reaction rates are usually controlled by the cathodic reaction and the availability of oxygen, because oxygen acts as an efficient depolariser. In fact, oxygen usually has two effects: it removes the polarizing layer of atomic hydrogen and it can react directly with the metal or metal oxide, thus increasing the corrosion rate. Dissolved oxygen is the primary oxidant in a new pipeline system. Sarin et al. (2003) studied iron release from a corroded unlined cast iron pipe considering the role of pH, alkalinity, and orthophosphate in controlling iron release and concluded that corrosion was sensitive to changes in alkalinity which itself was closely linked to turbidity, and turbidity was directly proportional to the iron concentration. In another study, a conceptual model was developed that described the formation and growth of iron scales and the reactions that lead to coloured water (Sarin et al., 2004).

Particularly through its influence on iron solubility, pH is another important parameter responsible for the variation of iron release rates in distribution systems. An increase in pH decreases the solubility of ferrous hydroxide and ferrous carbonate (siderite) thus reducing the rate of iron release. The corrosion rate of mild steel is a function of pH and buffer capacity and, as the buffer capacity decreases with increasing pH, the corrosion rate will decline (Pisigan and Singley, 1987). One study, Larson (1966), concluded that an increase in alkalinity generally leads to diminished corrosion rates; a similar kind of result was obtained by Sarin et al. (2004). Reduced customer complaints of red water have been correlated with higher alkalinity (Horsley et al., 1998).

The carbonate system is one of the most important components in all aquatic environments, because it directly affects pH which in turn influences the concentrations of other chemical species. Among carbonate species, carbon dioxide is the most important and is responsible for much of the corrosion of iron pipes (Sanders et al., 1996). Dissolved carbon dioxide accelerates the dissolution of iron in aqueous solution by destabilizing the oxide films. This dissolution process produces ferrous carbonate and a dissolved complex of iron (Linter and Burstein, 1999). The iron complexes that are formed by electrochemical reactions can establish either protective or non protective layers depending on the conditions under which they are formed. Song et al. (2002) investigated the CO_2 corrosion of pipelines with different carbon dioxide concentrations and showed that the formation of FeCO_3 and $\text{Fe}(\text{OH})_2$ precipitation depends on available CO_2 concentration.

Several models have been developed to study corrosion in water distribution systems. Some of these models are the Heyer's Calcite Model, the Siderite (FeCO_3) Model, the Kuch and Wagner Model, the Discolouration Model, and the 2-D Multi-Component Corrosion Model. In 1888 Heyer undertook a comprehensive study of lead pipe corrosion and correlated the high concentration of dissolved carbon dioxide with the high lead concentration in the distribution water (Benjamin et al., 1996). Later, Tillmans et al. (1927), Langelier (1936) and Larson and Skold (1957) further modified this model. Larson and Skold further demonstrated the failure of Langelier Index and showed that no reliable correlation exists between the corrosion rate and the bulk water Langelier Index.

Sontheimer, Kölle and Rudek (1979) introduced a Siderite model as an alternative to the Calcite model, based on the concept that the formation of siderite (FeCO_3) is most important for the creation of a protective layer (Sontheimer et al., 1981). The authors described their model using three sets of chemical reactions. Kuch and Wagner (1983) used a mass transport model to investigate lead concentration in pipes during steady state conditions. Kuch further investigated the reduction and re-oxidation kinetics of iron oxide scales and concluded that iron oxide formed during corrosion can be reduced by dissolution of metallic iron during unsteady conditions (Kuch, 1988). Refait et al. (1997 and 1998) conducted a detailed study into the role of various green rust compounds in the corrosion process. Tanggara (2004) studied the iron release process in dead ends of a water distribution system through a multi-component chemical model.

A recent work on corrosion highlights the discolouration process in a potable water supply networks (Boxall and Saul, 2005). The authors developed, verified and validated a cohesive transport modeling approach to simulate the discolouration process within distribution systems. Another recent contribution is a 2D multi-component corrosion model by Naser and Karney (2005) which numerically simulates the concentration of chemicals in water distribution systems during different flow conditions, both in the axial and radial directions. The reactions, which take place either in the bulk flow or at the pipe wall, release chemicals into the system. This study also explores the effect of pH and the initial concentration of dissolved oxygen on the corrosion process. Naser and Karney (2005) also proposed a 1-D corrosion model in which the corrosion terms are averaged in the radial direction. All the governing equations are conceptually the same as in the 2-D model and the combination of the implicit finite difference method and the method of characteristics is used to solve the system equations.

The purpose of the current paper is to investigate the impact of various chemical and physical parameters in an extended 1-D corrosion model for transient conditions. The combination of the corrosion process and the hydraulic turbulent mechanism further bolsters the already high potential for water quality deterioration. Turbulence affects a water distribution system in two ways. Firstly, it permits a high transfer rate of oxygen to the pipe wall which is responsible for oxidization of the pipe material. Secondly, the shear stress developed due to turbulence efficiently transfers corroded materials to the bulk flow. Dealing with the different factors governing corrosion and their impact on water quality remains a challenging question demanding further research and investigation.

2. EXTENSION OF THE 1-D MULTI-COMPONENT CORROSION MODEL

This research is focused on the extension of an existing 1-D transient corrosion model (Naser and Karney, 2005) to study the impact of various chemical species— dissolved oxygen (DO), pH, and carbonate system (CO_2 , HCO_3^- , & CO_3^{2-}) on the formation of ferrous (Fe^{2+}) and ferric (Fe^{3+}) ions. Along with this study, the associated formation of various iron precipitates is also numerically explored. Each chemical species is tracked using the advection-diffusion-reaction equation (ADRE) which is solved by the implicit finite

difference method. This chemical modelling component (i.e., the ADRE equation) is coupled with the transient hydraulic modelling component to track the concentration of constituents.

2.1 Hydraulic Component of the Model

An effective and accurate hydraulic model is a prerequisite for an effective and accurate corrosion or any other water quality model. Transient analysis is not simple, because the governing equations describing them are of the non linear and partial differential variety; the hydraulic devices are complex and it is difficult to obtain usual performance data for them. Two fundamental equations, a momentum equation and continuity equation are used to model one dimensional transient flow in a pipeline (Wylie and Streeter, 1993 and Chaudhry, 1987). If x is distance along the centreline of the conduit, t is time, and partial derivatives are represented as subscripts, then the pair of equations can be written as:

$$V_t + gH_x + \frac{f}{2D} V |V| = 0 \quad (1)$$

$$\frac{g}{a^2} H_t + V_x = 0 \quad (2)$$

where, $H = H(x,t)$ = piezometric Head, $V = V(x,t)$ = flow velocity, a = wave speed, f = Darcy-Weisbach friction factor, D = internal pipe diameter, g = acceleration due to gravity, and V_x , H_x , V_t , H_t are the partial derivative of flow velocities and heads with respect to time and distance.

The momentum (1) and continuity (2) equations form a pair of quasi-linear hyperbolic partial differential equations in terms of two dependent variables, velocity and piezometric head, and two independent variables, distance along the pipe and time. In this hydraulic model, these two partial differential equations are solved using the method of characteristics and the chemical transport through an implicit finite difference method.

2.2 Development of the Chemical Corrosion Model

The internal corrosion of the pipe wall can be influenced by the transport of different chemical species including dissolved oxygen, pH (the hydrogen ion), ferrous and ferric ions, and the carbonate species (CO_2 , HCO_3^- and CO_3^{2-}). For the comprehensive corrosion analysis, it is necessary to address the advection and longitudinal dispersion of chemical species under all flow conditions. Thus, the mass transport of chemical species as well as iron liberated from the pipe wall can be efficiently described with the following a second order parabolic partial differential equation, commonly known as the advection-diffusion-reaction equation (ADRE).

$$\frac{\partial C_{(x,t)}}{\partial t} + U_{(x,t)} \frac{\partial C_{(x,t)}}{\partial x} = D \frac{\partial^2 C_{(x,t)}}{\partial x^2} \pm S_t(C_{(x,t)}) \quad (3)$$

where C is the concentration of chemical specie at (x, t) and $S_t(C)$ represents the source/sink term defining the consumption or release of chemical specie during corrosion. The second term on left side represents the advection term, which accounts for the migration of chemical species in the bulk flow. The first term on the right hand side accounts for the diffusion of chemicals in the longitudinal direction and the last term accounts for growth/decay of the chemical constituent due to its reaction with substances in the bulk flow or at the pipe wall; this is also called the source/sink term. The 1-D hydraulic model described in section (2.1) is coupled with the ADRE to analyse the concentration of each chemical ion released to the

water. The implicit formulation of the ADRE is based on the algorithm presented by Fernandes and Karney (2004) with slight variation because of the consideration of source/sink term.

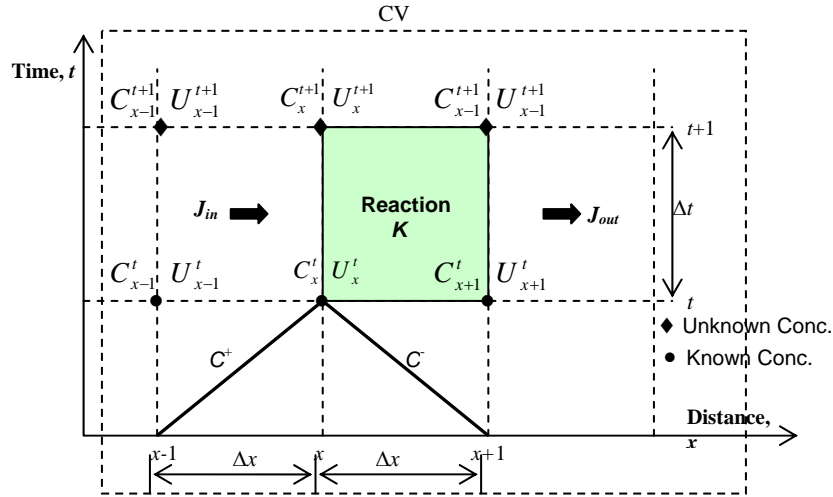


Figure 1: x - t grid for ADRE solution

The ADRE is solved numerically by the implicit finite difference method. Figure 1 represents the x - t grid and control volume definition for the solution of ADRE, i.e. equation (3). The grid point (x, t) represents the location at position x and time t . The x - t grid is defined based upon the MOC procedure which serves as the basis for establishing the finite difference approximation to represent the derivatives in the partial differential equation. As described in Fernandes and Karney (2004), the upstream boundary condition is defined as a Dirichlet boundary and the initial concentration $C_{(x, 0)}$ of the constituent is assumed known.

If J_{in} is the flux of constituent mass entering the control volume, J_{out} is the mass flux leaving the control volume, \underline{V} is the influenced volume ($\underline{V} = A \cdot \Delta x$), then the mass balance within the control volume can be expressed as,

$$\underline{V} \frac{\partial C}{\partial t} = (J_{in} - J_{out})A + K \underline{V} C$$

and the following implicit finite difference expression is formulated for the ADRE:

$$I_3 C_{x-1}^{t+1} + I_4 C_x^{t+1} + I_5 C_{x+1}^{t+1} = I_1 C_{x-1}^t + I_2 C_x^t + I_6 C_{x+1}^t \quad (4)$$

where C is the concentration of the k^{th} -chemical at a different nodal point in the finite difference grid, and the known coefficients I_1, I_2, I_3, I_4, I_5 and I_6 are defined as follows:

$$\begin{aligned} I_1 &= 1 + \frac{\Delta t}{\Delta x} U_{x-1}^t + K \frac{\Delta t}{2} + D_{x-1}^t \frac{\Delta t}{\Delta x^2}, & I_2 &= 1 - \frac{\Delta t}{\Delta x} U_x^t + K \frac{\Delta t}{2} - 2D_x^t \frac{\Delta t}{\Delta x^2} \\ I_3 &= 1 - \frac{\Delta t}{\Delta x} U_{x-1}^{t+1} - K \frac{\Delta t}{2} - D_{x-1}^{t+1} \frac{\Delta t}{\Delta x^2}, & I_4 &= 1 + \frac{\Delta t}{\Delta x} U_x^{t+1} - K \frac{\Delta t}{2} + 2D_x^{t+1} \frac{\Delta t}{\Delta x^2} \\ I_5 &= -D_{x+1}^{t+1} \frac{\Delta t}{\Delta x^2}, & I_6 &= D_{x+1}^t \frac{\Delta t}{\Delta x^2} \end{aligned}$$

The turbulent diffusion coefficient D at any nodal point is related to the velocity and friction factor by the following relation, which was developed using Taylor's approach:

$$D_x = \left| 10.1 \times r \times U \times \sqrt{\frac{f}{8}} \right|$$

where r = radius of the pipe and U = flow velocity.

The equation (4) is converted into a tri-diagonal equation to calculate the concentration of the k^{th} -chemical at a different nodal point at time level $t+1$. This tri-diagonal equation forms a tri-diagonal matrix which is then solved by the Thomas algorithm (Naser, 2006).

$$A_L C_{K,x-1}^{t+1} + A_D C_{K,x}^{t+1} + A_U C_{K,x+1}^{t+1} = F_K$$

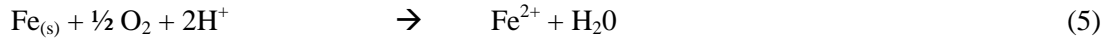
This equation in matrix form could be expressed as $A \times C_x = F_K$, in which A represents the coefficients of each term on the right side and F_K is the sum of all the right side terms of equation (4), which are known.

2.3 Chemical Reactions with the Pipe Wall

Corrosion is the most common form of metallic degradation due to the electro-chemical interaction between a metal surface and its environment. During the corrosion process, two simultaneous reactions occur at the anode and cathode.

(a) Basic Corrosion Reaction

At the anodic region iron in the bulk water generates electrons, while in the cathodic area, the electrons generated in the anode are used in the reduction of oxygen.



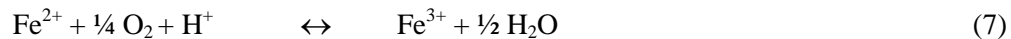
The reaction (5) is assumed to be irreversible and the rate of changes of chemical species due to this reaction is governed by

$$\frac{\partial[\text{Fe}^{2+}]}{\partial t} = -2 \frac{\partial[\text{O}_2]}{\partial t} = -\frac{1}{2} \frac{\partial[\text{H}^+]}{\partial t} = K_1 [\text{O}_2]^{n_1} [\text{H}^+]^{n_2} [\text{Fe}^{2+}]^{n_3} \quad (6)$$

where, K_1 is the reaction rate constant, n_1 , n_2 and n_3 are the orders of reaction for oxygen, hydrogen ion (pH) and ferrous ion, respectively.

(b) Extension of the Basic Reaction with Ferric (Fe^{3+}) ion

In the presence of dissolved oxygen, Fe^{2+} further oxidizes into Fe^{3+} ion.



It is most likely that ferric ion reduces back to ferrous ion because of many environmental circumstances. So, utilizing both forward and backward rate constants:

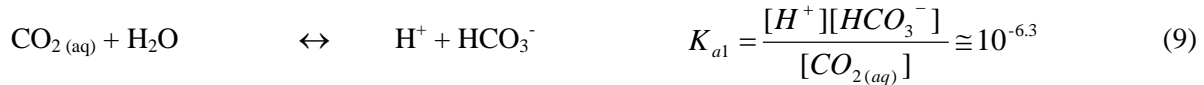
So, the rate of change of chemical species in reaction (7) can be written as:

$$\frac{\partial[\text{Fe}^{3+}]}{\partial t} = -\frac{\partial[\text{Fe}^{2+}]}{\partial t} = -4 \frac{\partial[\text{O}_2]}{\partial t} = -\frac{\partial[\text{H}^+]}{\partial t} = K_{2f} [\text{O}_2]^{n_1} [\text{H}^+]^{n_2} [\text{Fe}^{2+}]^{n_3} - K_{2b} [\text{Fe}^{3+}]^{n_3} \quad (8)$$

(c) Inclusion of the Carbonate System

The carbonate system is one of the key components of the corrosion process in aquatic environments. This is because the dissolution and precipitation of iron species also depend on the presence of carbonate species in solution, and a considerable buffering action can take place. In particular, the carbonate system plays an important role in neutralizing acids and bases thereby controlling solution pH. Therefore, the chemistry of many important reactions is influenced by the presence of carbonate species. The chemical species that make up the carbonate system in a water distribution network are aqueous carbon dioxide ($CO_{2(aq)}$), carbonic acid ($H_2CO_3^*$), bicarbonate (HCO_3^-) and carbonate (CO_3^{2-}). The inclusion of the carbonate system in the water corrosion model brings the model closer to the chemistry of the actual system.

Stumm and Morgan (1996) stated that the rate of carbonic acid ionization is more rapid than its formation and that its concentration is negligible compared to the concentration of aqueous carbon dioxide (Snoeyink and Jenkins, 1980). In most analytical procedures, it is also difficult to distinguish $CO_{2(aq)}$ from H_2CO_3 . Therefore, a composite dissociation reaction is as follows:



where K_{a1} and K_{a2} are the dissociation constants involved in reactions (9) and (10).

The changes of concentrations of chemical species involved in reactions (9) and (10) with time can be determined by the following reaction kinetics:

$$-\frac{\partial[CO_2]}{\partial t} = \frac{\partial[H^+]}{\partial t} = \frac{\partial[HCO_3^-]}{\partial t} = K_{3f}[CO_{2(aq)}] - K_{3b}[H^+][HCO_3^-] \quad (11)$$

$$\frac{\partial[CO_3^{2-}]}{\partial t} = \frac{\partial[H^+]}{\partial t} = -\frac{\partial[HCO_3^-]}{\partial t} = K_{4f}[HCO_3^-] - K_{4b}[H^+][CO_3^{2-}] \quad (12)$$

where K_{3f} , K_{3b} , K_{4f} and K_{4b} are the forward and backward reaction rates.

The initial concentration of carbonate species involved in the above reactions is determined from the total carbonate concentration (C_T).

$$C_T = [CO_{2(aq)}] + [H_2CO_3] + [HCO_3^-] + [CO_3^{2-}] \cong [CO_{2(aq)}] + [HCO_3^-] + [CO_3^{2-}] \quad (13)$$

Since the entire system is considered closed, the C_T concentration will not change during the entire simulation process. The initial concentration of each carbonate species is calculated from the ionization fractions of the total carbonate system according to the following equations:

$$[CO_{2(aq)}]_{(t,x=0)} = \alpha_0 C_T; \quad [HCO_3^-]_{(t,x=0)} = \alpha_1 C_T \quad \text{and} \quad [CO_3^{2-}]_{(t,x=0)} = \alpha_2 C_T$$

where α_0 , α_1 , α_2 are the ionization fraction coefficients which are a function of the dissociation constants and pH of the solution.

(d) Inclusion of the Precipitation Model

The ferrous and ferric ions released into the water often further react with hydroxide, carbonate or other anions present in the bulk water and may undergo a number of secondary reactions. Depending on the solubility products and various concentrations, such reactions could lead to precipitation. Although there are many possible precipitation reactions, in the present model, precipitation of ferrous hydroxide $[Fe(OH)_2]$ and siderite $[FeCO_3]$, which are considered important in iron corrosion, is represented with following chemical reactions.

Precipitation of Siderite:



Siderite precipitation in the system could only be possible (Stumm and Morgan, 1996), if

$$[Fe^{2+}] [CO_3^{2-}] \geq K_{sp1}$$

This gives an equilibrium concentration of Fe^{2+} for siderite precipitation as:

$$[Fe^{2+}]_{eq} = \frac{K_{sp1}}{[CO_3^{2-}]^2}$$

Precipitation of Ferrous Hydroxide:



The same approach is used for siderite to calculate the equilibrium concentration of ferrous ion for ferrous hydroxide precipitation. Therefore, in order to form $Fe(OH)_2$, the following condition should be met (Stumm and Morgan, 1996):

$$[Fe^{2+}] [OH^-]^2 \geq K_{sp2}$$

which gives an equilibrium concentration of iron for $Fe(OH)_2$ precipitation as:

$$[Fe^{2+}]_{eq} = \frac{K_{sp2}}{[OH^-]^2}$$

Since the model focuses on the iron release phenomenon, the rate of formation of siderite and ferrous hydroxide is expressed, from reaction (14) and (15), as:

$$\frac{\partial [FeCO_3]}{\partial t} = K_{s1} \cdot [Fe^{2+}]^{n_3} [CO_3^{2-}]^{n_4} \quad (16)$$

$$\frac{\partial [Fe(OH)_2]}{\partial t} = K_{s2} \cdot [Fe^{2+}]^{n_3} [OH^-]^{n_2} \quad (17)$$

where K_{s1} and K_{s2} are reaction rate constants for siderite and ferrous hydroxide respectively.

The order of reaction is set as a pseudo-first order with respect to oxygen and pH and pseudo-zero order with respect to iron. This means that the concentrations of other chemical species are assumed constant while calculating the rate of chemical change one specific substance. So, in the expressions (6), (8), (16) and (17) the coefficients $n_1 = n_2 = n_4 = 1$ and $n_3 = 0$.

The source/sink terms (S_i) for the ADRE model (equation 3) are obtained from the combination of expressions (6), (8), (11), (12), (16) and (17). The source/sink terms of each chemical species from all these expressions are combined and incorporated in the ADRE. All together, nine source/sink terms are included in the model and their influence on iron release in a water distribution system is studied.

3. CASE STUDY

The system consists of two constant head reservoirs as depicted in Figure 2 connected by pipeline that is 1000 m long, 1128.4 mm in diameter and has a Darcy-Weisbach friction factor of 0.05 and a wavespeed of 1000.0 m/s. The water levels in the upstream and downstream reservoirs are 200 m and 180 m, respectively. When the valve is fully opened, the steady state flow rate is 2000 l/s.



Figure 2: Schematic of the pipe system

The effective headloss coefficient of the downstream valve is considered to be $E_s = 0.604 \text{ m}^{2.5}/\text{s}$. Initially, the valve is fully closed and there is no flow, then the valve is suddenly opened to introduce a transient into the system. Initial concentrations of ferrous and ferric ion are considered as zero. For simulation purposes, the pipe is divided lengthwise into 400 reaches giving a mesh size of 2.5 m and a time step of 0.0025 s.

The following boundary and initial conditions are used to study iron release in this case study.

At the upstream (Inlet) section, a constant head reservoir is assumed for the hydraulic model and a boundary with constant concentration is assumed for the corrosion model

$$C_K(x, t = 0) = C_{k_{in}}, \text{ where } C_K \text{ is the concentration of } K^{\text{th}} \text{ chemical species.}$$

At the downstream section, a valve is assumed to exist for the hydraulic model and a no flux boundary for all species is applied in the corrosion model.

$$\left. \frac{\partial C_K}{\partial t} \right|_{x=L} = 0.0$$

Initial Conditions: This deals with the concentration of each chemical species prior to, and at the onset of, the transients in which species concentrations are spatially uniform throughout the system; that is, the concentration for a given constituent is the same at all nodes for $t = 0$

4. RESULTS AND DISCUSSIONS

Ferrous and ferric ion release phenomena are carefully analyzed in the present model. Figure 3 compares iron release into the bulk flow in the basic model at 300 s and 3600 s after valve opening. This result shows that iron release at 300 s is not as fully developed in comparison with a simulation time of 3600 s.

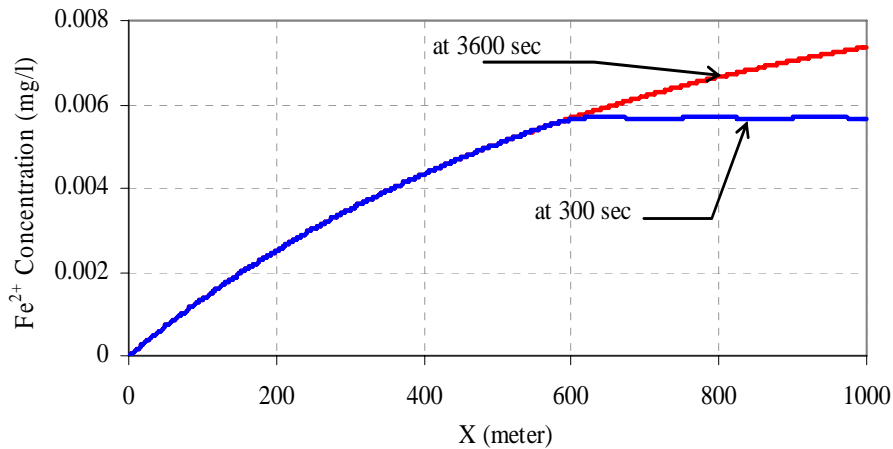


Figure 3: Iron concentration into the bulk flow along the pipeline (Basic Model)

Figure 4 interprets the result after the extension of the basic model with the inclusion of ferric ion ionization. Ferrous ion is further oxidized into ferric ion in the presence of dissolved oxygen.

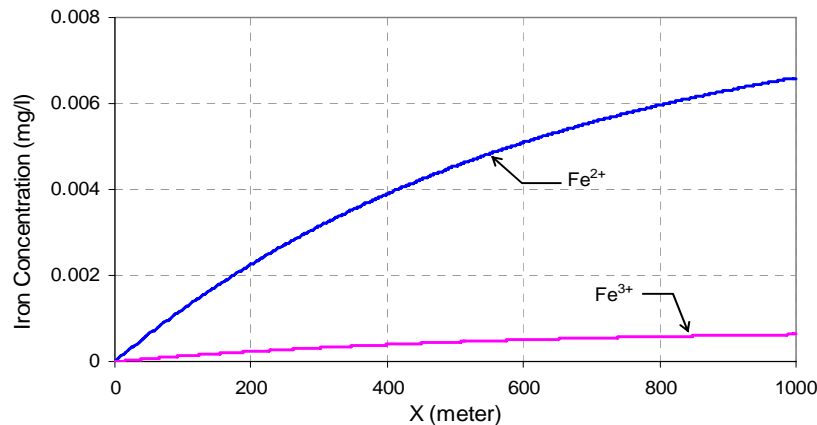


Figure 4: Iron concentration (Fe^{2+} and Fe^{3+}) at 3600 s of simulation

The extent of ferric ion formation mostly depends on the rate at which the ferrous ions are further ionized into ferric ions. The total amount of ferrous ions decreased in the bulk solution, as related in Figure 5, when some the ferrous species is ionized into ferric ions.

Figures 6 and 7 summarize the changes in DO concentration and pH values along the pipe axis after 300 s and 3600 s of simulation time. The results indicate that the DO concentration is decreasing and pH is increasing along the pipe axis, in agreement with the Naser-Karney model. However, in a real distribution system the result may be different because of the effect of the carbonate system and other possible secondary chemical reactions.

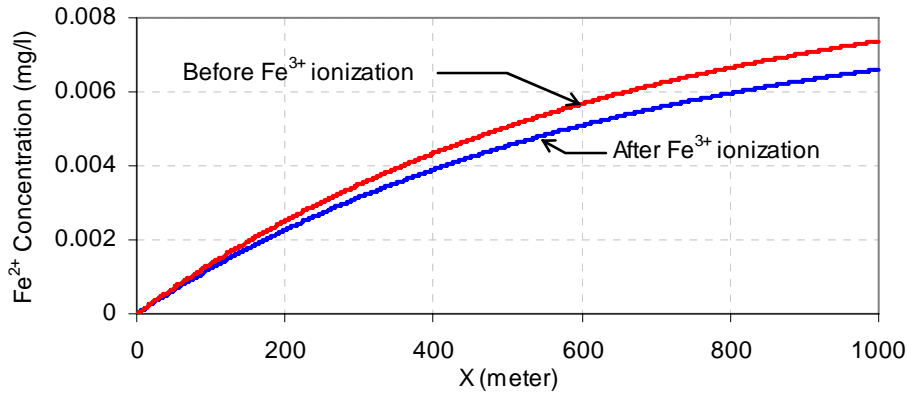


Figure 5: Change in Fe^{2+} concentration after Fe^{3+} ionization at 3600 s of simulation

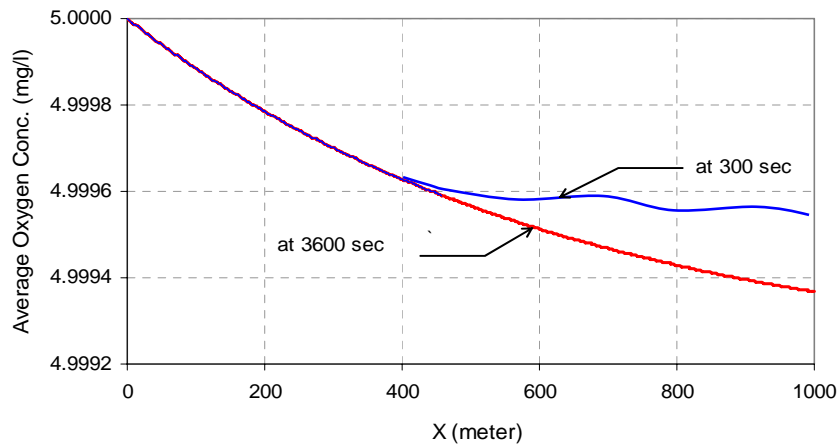


Figure 6: Oxygen consumption along the pipe axis

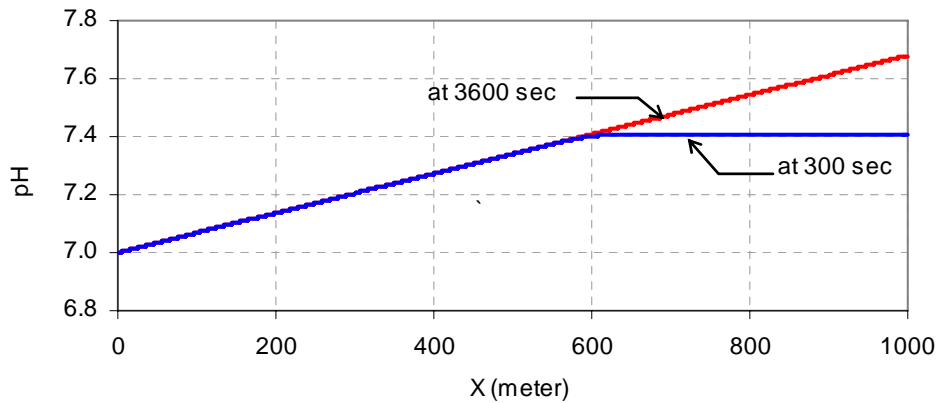


Figure 7: Change in solution pH along the pipe axis

Although there is no direct relationship between the carbonate system and iron release, it clearly affects the pH of the system. The simulation, as summarized in Figure 8, demonstrates that iron release in the system increases after the inclusion of the carbonate system. This is mainly due to the decrease of pH and the contemporaneous increase of DO concentration and reveals that there is a notable impact of the carbonate system on corrosion in a water distribution system.

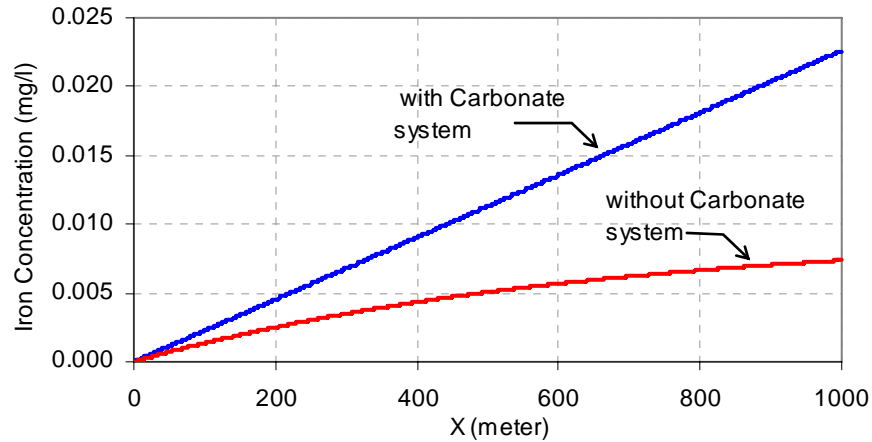


Figure 8: Comparison of iron release with and without carbonate system at 600 s

Figures 9 and 10 follow the changes in dissolved oxygen concentration and pH after inclusion of the carbonate system at 600 s simulation time. It is evident that pH is decreasing and DO concentration is increasing longitudinally, ultimately augmenting iron release from the system. Comparing these figures (i.e., Figures 9 and 10) with Figures 6 and 7, DO and pH manifest exactly the opposite behaviour in the presence of the carbonate system.

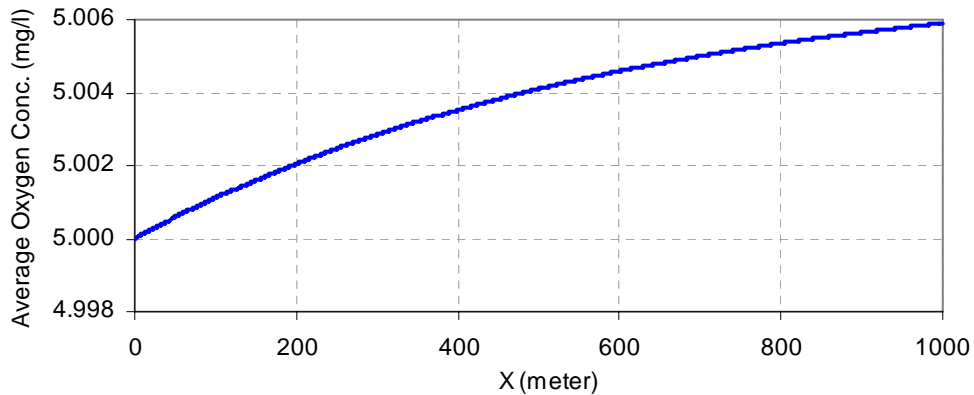


Figure 9: Change in DO concentration after inclusion of the carbonate system

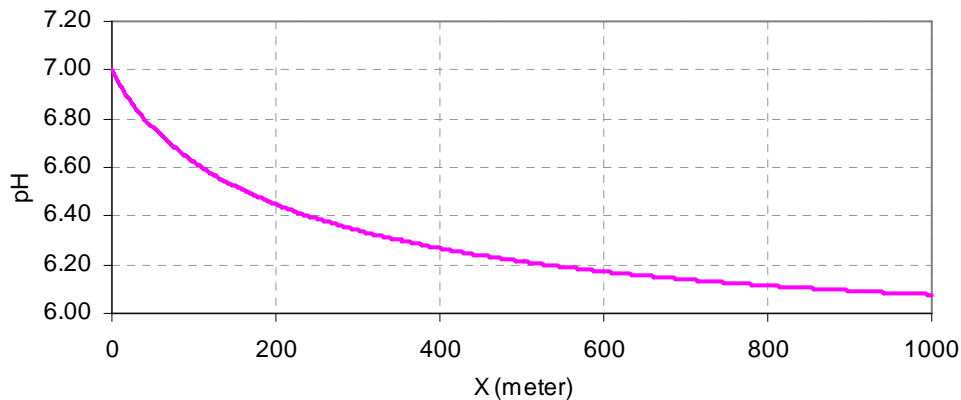


Figure 10: Change in pH of water after inclusion of the carbonate system

The variation of DO and pH after inclusion of the carbonate system is also proved by the alteration of the carbonate species along the pipe axis. Figures 11 and 12 document the changes of the carbonate species after one hour of simulation and these figures show that bicarbonate and carbonate concentrations are declining along the axis, thus reducing the alkalinity of the water. This verifies the decrease of pH along the axis as presented in Figure 10. Hence, a drop in pH, and a rise in DO concentrations along the pipe axis, which are observed following the inclusion of the carbonate system in the model, accelerate oxidation of the pipe wall and boost the iron release rate along the pipe axis.

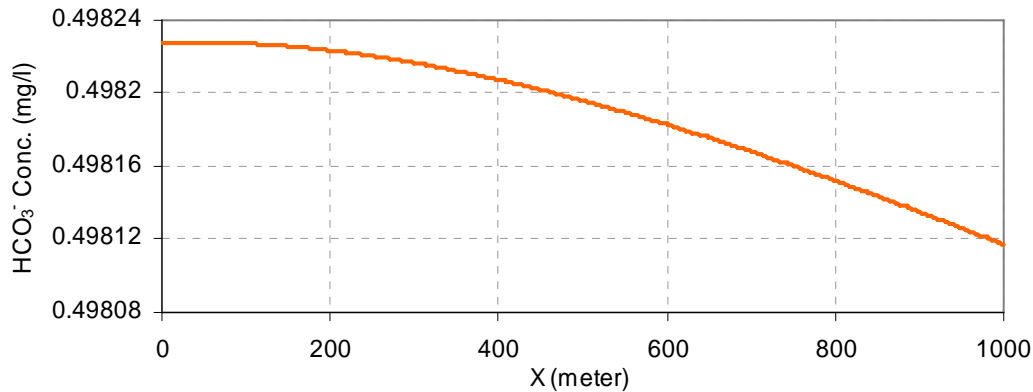


Figure 11: Bicarbonate (HCO_3^-) concentration along the pipe axis at 3600 sec

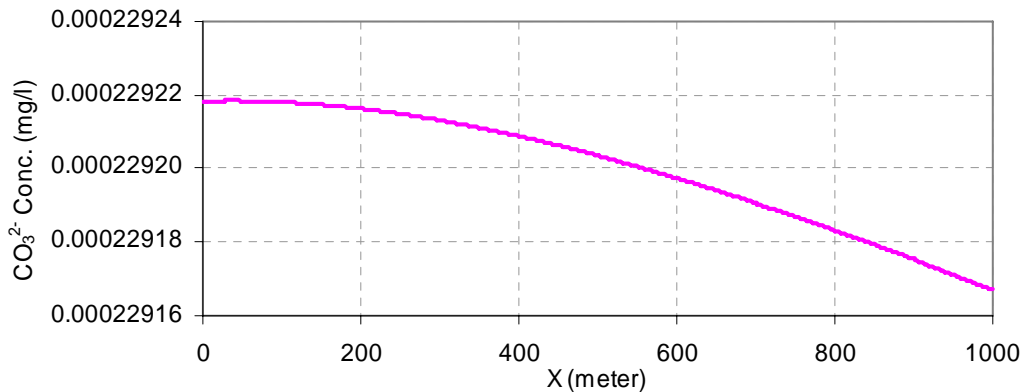


Figure 12: Aqueous CO_2 Concentration along the pipe axis at 3600 sec

The effect of the initial concentration of DO and pH has also been investigated in this model, and it is found that the initial pH value exerts a strong influence on iron release. As the initial pH value diminishes, the more acidic water produces a strong electro-chemical influence in the system that exacerbates iron release. According to Wagner (1993), at low pH, a high concentration of H^+ ions serves as an additional oxidant in the system that aggravates corrosion, something corroborated by this simulation result as well. Comparing the results with respect to initial DO and pH for same hydraulic conditions, the influence of initial pH is greater than the influence of initial DO concentration which agrees with the result obtained by the 2-D model of Naser and Karney (2005).

A number of secondary reactions occur between the ferrous and ferric ions released into the water with hydroxide, carbonate or other anions present in the bulk water which could possibly yield various

precipitates. The potential for ferrous hydroxide and ferrous carbonate (siderite) precipitation is explored in this model. Figures 13 and 14 show the formation of siderite and ferrous hydroxide precipitation respectively.

These precipitates depend on various factors such as forward and backward reaction rates, solubility product concentration, anion concentration, etc. Siderite precipitation occurs in the presence of the carbonate system exclusively, and it occurs only if the solubility product concentration is greater than or equal to $10^{-10.7} \text{ mole}^2/\text{l}^2$ (Stumm and Morgan, 1996). This points to a more or less a linear relationship governed in the formation of siderite precipitation.

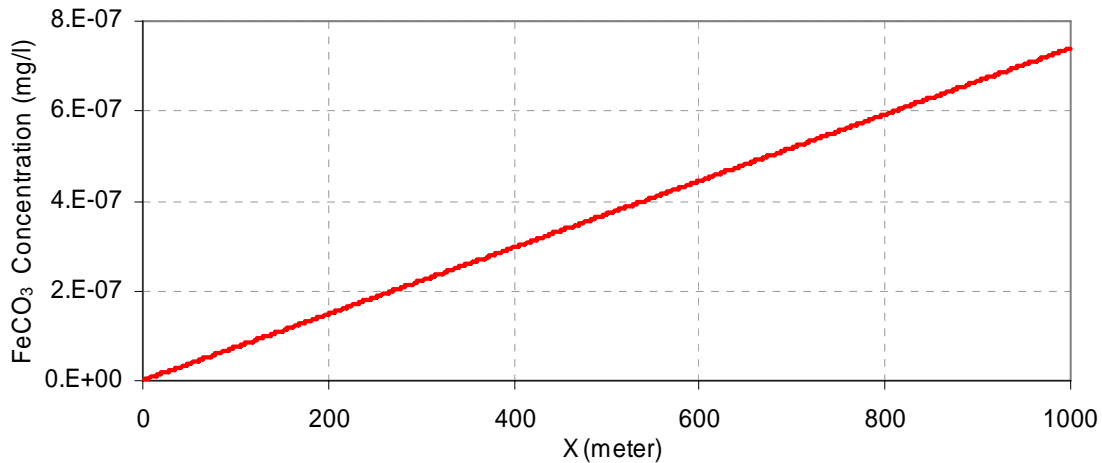


Figure 13: Siderite Precipitation at 3600 s of simulation

Figure 14 depicts the trend of ferrous hydroxide precipitation formation. For the given conditions, the figure reveals that $\text{Fe}(\text{OH})_2$ precipitation occurs only in the initial section of the pipe axis (i.e., close to the upstream section). Because of the limitation of solubility product concentration, ferrous hydroxide precipitation does not occur after that stage and proceeds only if the solubility product concentration is greater than or equal to $10^{-14.7} \text{ mole}^3/\text{l}^3$ (Stumm and Morgan, 1996). The reason is that pH decreases slowly along the axis due to inclusion of the carbonate system, with ferrous hydroxide precipitation being observed due to higher OH^- concentrations in the upstream portion of the pipe.

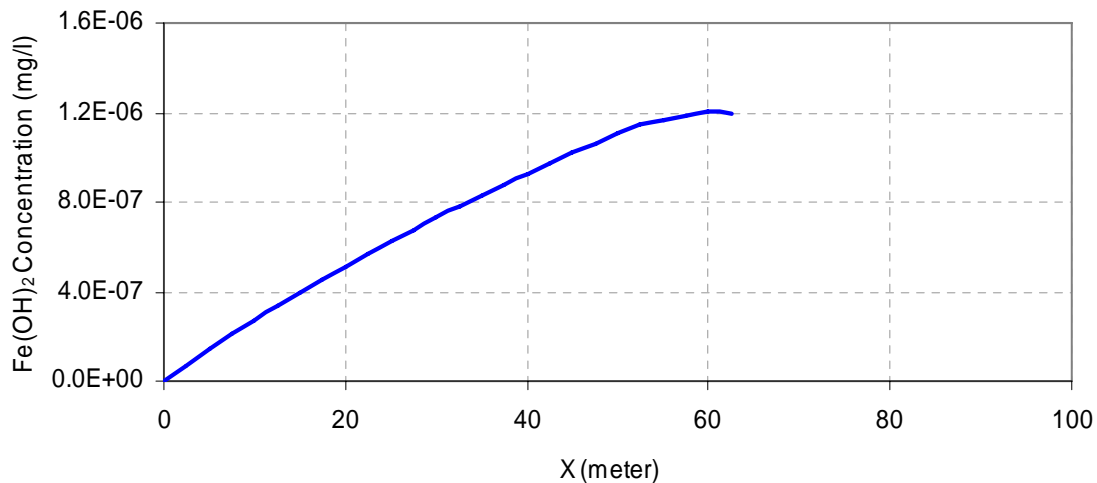


Figure 14: Ferrous Hydroxide Precipitation at 3600 s of simulation

5. CONCLUSIONS

Corrosion is a protracted phenomenon in the water distribution system which unfolds over years and decades. In this sense the current study is a highly preliminary explanation which merely attempts to envision some apparent trends of pipe corrosion. Yet, in this context, and with this proviso, a few preliminary and tentative conclusions are possible.

This study clearly reveals that DO and pH values significantly influence the iron release rate of metallic pipe. The study shows that higher DO concentration and lower pH produce a higher iron release rate, with the initial concentrations of DO and pH exerting a pronounced influence. An increase of initial DO concentration, or decrease of initial pH level, leads to a higher iron release rate; however, the effect of initial DO concentration is comparatively smaller than that of initial pH. Therefore, it can be concluded that a considerably higher pH is more beneficial for minimizing iron release from the pipe. The release of ferric ions depends on the reaction rate and on the amount of ferrous ions in the solution. Although it was found that the release of ferric ions increases along the axis, it is always less than for ferrous ions.

The effect of carbonate concentration in the corrosion process is obvious since it helps govern the pH of the system. The simulation result demonstrates that iron release in the system is increased after the inclusion of the carbonate system. This is mainly due to the decrease of system pH and the increase of dissolved oxygen concentration. Modelling of the species of the carbonate systems (i.e., aqueous CO_2 , HCO_3^- and CO_3^{2-}) evinced a decreasing trend of bi-carbonate and carbonate concentration along the axis, which verifies the reduction of pH along the axis. Therefore, the decrease in pH and increase in DO concentration along the pipe axis resulting from inclusion of the carbonate system in the model accelerate the oxidation of the pipe wall, and a high rate of iron release is observed along the pipe axis.

Finally, the possibility of ferrous hydroxide and ferrous carbonate (siderite) precipitation is also addressed in the model. These precipitates depend on various factors such as forward and backward reaction rates, solubility product concentration, and anion concentrations. The results suggest that there is an almost linear relationship in the formation of siderite precipitation; however, for the given conditions, a non-linear relationship of $\text{Fe}(\text{OH})_2$ precipitation (which was due to higher OH^- concentration) was found only in the initial stage (close to upstream portion) of pipe axis.

References

- Benjamin et al. (1996). *Internal Corrosion of Water Distribution Systems*. 2nd Edition, AWWA Research Foundation, Denver, USA.
- Boxall, J.B. and Saul, A.J. (2005). "Modeling discolouration in potable water distribution system". *J. of Environmental Engineering*, ASCE, 131 (5), 716-725.
- Chaudhry, M.H (1987). *Applied Hydraulic Transients*. 2nd Edition, Van Nostrand Reinhold, New York, USA.
- Fernandes, C. and Karney, B.W. (2004). "Modelling the advection equation under water hammer conditions". *Urban Water Journal*, 1(2), 97-112
- Geldreich, Edwin (1996). *Microbial quality of water supply in distribution systems*. Lewis Publishers, New York.
- Grayman, W., Rossman, L., and Geldreich, E. (2000). "Water quality". In: *Water Distribution System Handbook* (Ed. Larry Mays), Chapter 11, McGraw Hill Publication.
- Horsley, M.B. et al. (1998). "Monitoring iron corrosion in a lime softened water". *Proceeding of 1998 AWWA WQTC*, San Diego, USA.

- Kuch, A. and Wagner, I. (1983). "A mass transport model to describe lead concentration in drinking water". *Water Resource*, 17(10), 1303-1307
- Kuch, A. (1988). "Investigations of the reduction and re-oxidation kinetics of Iron(III) oxide scales formed in water". *Corrosion Science*, 28 (3), 221-231.
- Langelier W. F. (1936), "The analytical control of anticorrosion water treatment", *J. of American Water Works Association*, 28, 1500-1521.
- Larson, T.E. (1966). "Deterioration of Water Quality in Distribution Systems." *Journal of American Water Works Association*, 58(10), 1307-1316.
- Larsen T. E. and Skold R. V., (1957), "Corrosion and tuberculation of cast iron", *J. of American Water Works Association*, 49, 1294.
- Linter, B.R. and Burstein, G.T. (1999). "Reactions of pipeline steels in carbon dioxide solutions". *Corrosion Science*, 41(1), 117-139.
- McNeill, L.S. and Edwards, M. (2001). "Iron pipe corrosion in distribution systems". *J. of American Water Works Association*, 93(7), 88-100.
- Naser, G. and Karney, B.W. (2005). "A numerical study of a 2D multi-component corrosion model in a water distribution system". *Proceeding of the 2005 World Water and Environmental Resources Congress*, Alaska, USA, 15-19 May, 2005.
- Naser, G. (2006). "Water quality in distribution systems: A two dimensional multi-component simulation model". *PhD Dissertation*, University of Toronto, Canada.
- Pisigan Jr. R.A. and Singley, J. E. (1987). "Influence of buffer capacity, chlorine residual and flow rate on corrosion of mild steel and copper". *Research and Technology*, 79(2), 62-70
- Refait, P.H., Abdelmoula, M., and Génin J.M.R (1998). "Mechanisms of Formation and Structure of Green Rusts in Aqueous Corrosion of Iron in the Presence of Chloride ions". *Corrosion Science*, 40(9), 1547-1560.
- Refait, P.H.; Drissi, S.H.; Pytkiewicz, D.J. and Génin, J.M.R. (1997). "The Anionic Species Competition in Iron Aqueous Corrosion: Role of Various Green Rust Compounds". *Corrosion Science*, 39(9), 1699-1710.
- Sander, A., Berghult, B., Broo, A.E., Johnasson, E.L., and Hedberg, T. (1996). "Iron corrosion in drinking Water distribution systems – The effects of pH, calcium and hydrogen carbonate". *Corrosion Science*, 38(3), 443-455.
- Sarin, P., Snoeyink, V.L., Lytle, D.A., and Kriven, W.W. (2004). "Iron corrosion scales: models for scale growth, iron release, and coloured water formation". *J. of Environmental Engineering*, ASCE, 130(4), 364-373.
- Sarin, P., Clement, J.A., Snoeyink, V.L., and Kriven, W.W. (2003). "Iron release from corroded unlined cast iron pipe". *J. of American Water Works Association*, 95(11), 85-96.
- Sarin, P., Soneyink, V.L., Bebee, J., Kriven, W.M., and Clement, J.A. (2001). "Physico-chemical characteristics of corrosion scales of old iron pipes." *Water Research*, 35(12), 2961-2969.
- Song, F.M., Kirk, D.W., Graydon, J.W., and Cormack, D.E. (2002). "CO₂ corrosion of pipelines under a disbonded coating in the presence of a precipitate". *The J. of Corrosion Science and Engineering*, 3(24).
- Sontheimer, H, Kölle, W. and Snoeyink, V. L. (1981). "The siderite model of the formation of corrosion-resistant scales", *Research and Technology, J. of American Water Works Association*, 73 (11), 572-579.
- Snoeyink, V.L. and Jenkins, D. (1980). *Water Chemistry*. 3rd ed., John Wiley & Sons, New York.
- Stumm, W. and Morgan, J.J. (1996). *Aquatic Chemistry: Chemical Equilibria and Rates in Natural Waters*, Wiley, New York.
- Tenggara, A. (2004). *Preliminary model of corrosion and iron release in a pipeline system*. M.A.Sc. Thesis, Civil Engineering Department, University of Toronto, Toronto, Canada
- Tillmans J., Hirsch P., and Weintraud W., (1927), "Die Korrosion von Eisen unter Wasserleitungswasser". *gwf-Das Gas und Wasserfach*, 70:845-849 (Cited in Benjamin et al.,1996).

Wagner, I (1993). "Influence of operating conditions on material and water quality in drinking water distribution systems". *Corrosion and Related Aspects of materials for Potable Water Supplies*, Ed. P. McIntyre and A.D. Mercer, Proceeding of Conference, London, UK, 1992

Wylie, E.B., and Streeter V. L. (1993). *Fluid Transients in Systems*. Prentice Hall, New Jersey.